BIOCHEMISTRY
including biophysical chemistry & molecular biology

Article

pubs.acs.org/biochemistry

Differential Activation of Intracellular versus Plasmalemmal CB_2 Cannabinoid Receptors

G. Cristina Brailoiu,[†] Elena Deliu,[‡] Jahan Marcu,[‡,§] Nicholas E. Hoffman,[∥] Linda Console-Bram,[‡] Pingwei Zhao,[‡,§] Muniswamy Madesh,[∥] Mary E. Abood,*[,‡,§] and Eugen Brailoiu*[,‡,⊥]

[†]Department of Pharmaceutical Sciences, Thomas Jefferson University School of Pharmacy, Philadelphia, Pennsylvania 19107, United States

[‡]Center for Substance Abuse Research, [§]Department of Anatomy and Cell Biology, [∥]Center for Translational Medicine, and [⊥]Department of Pharmacology, Temple University School of Medicine, Philadelphia, Pennsylvania 19140, United States

Supporting Information

ABSTRACT: The therapeutic and psychoactive properties of cannabinoids have long been recognized. The type 2 receptor for cannabinoids (CB_2) has emerged as an important therapeutic target in several pathologies, as it mediates beneficial effects of cannabinoids while having little if any psychotropic activity. Difficulties associated with the development of CB_2-based therapeutic agents have been related to its intricate pharmacology, including the species specificity and functional selectivity of the CB_2-initiated responses. We postulated that a plasmalemmal or subcellular location of the receptor may contribute to the differential signaling pathways initiated by its activation. To differentiate between these two, we used extracellular and intracellular administration of CB_2 ligands and concurrent calcium imaging in CB_2-expressing U2OS cells. We found that extracellular administration of anandamide was ineffective, whereas 2-arachidonoyl glycerol (2-AG) and WIN55,212-2 triggered delayed, CB_2-dependent Ca^{2+} responses that were Gq protein-mediated. When microinjected, all agonists elicited fast, transient, and dose-dependent elevations in intracellular Ca^{2+} concentration upon activation of Gq-coupled CB_2 receptors. The CB_2 dependency was confirmed by the sensitivity to AM630, a selective CB_2 antagonist, and by the unresponsiveness of untransfected U2OS cells to 2-AG, anandamide, or WIN55,212-2. Moreover, we provide functional and morphological evidence that CB_2 receptors are localized at the endolysosomes, while their activation releases Ca^{2+} from inositol 1,4,5-trisphosphate-sensitive- and acidic-like Ca^{2+} stores. Our results support the functionality of intracellular CB_2 receptors and their ability to couple to Gq and elicit Ca^{2+} signaling. These findings add further complexity to CB_2 receptor pharmacology and argue for careful consideration of receptor localization in the development of CB_2-based therapeutic agents.

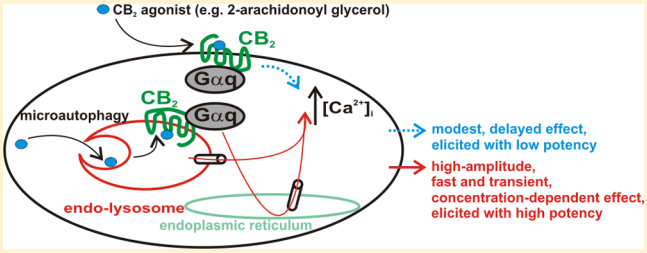

Although cannabinoids are active at several G protein-coupled receptors and ion channels, only two "true" cannabinoid receptors are recognized, namely CB_1 and CB_2.[1] Interest in the latter has sparked as it appeared as an important therapeutic target in inflammatory and painful conditions,[2,3] while not being involved in the psychoactive cannabinoid effects, which are mainly CB_1-mediated. As such, increasing effort is being spent in the development of CB_2-based therapeutic agents.[4,5] Nonetheless, controversies exist, for instance, in CB_2 pharmacology and distribution.[6−8] At least two CB_2 receptor isoforms have been identified, with tissue- and species-specific expression patterns.[8,9] It has been found that CB_2 agonists may elicit distinct responses at CB_2 receptors from different species.[10] Moreover, functional selectivity, defined as the ability of a receptor to couple to different signaling pathways depending on the ligand that stimulates it,[11] has been reported for CB_2.[7] Further complexity is added to the CB_2 receptor pharmacology with the recent finding that their intracellular activation modulates neuronal function.[12] Because CB_2 receptors have been found to signal through Ca^{2+},[12−15] we used calcium imaging and extracellular and intracellular administration of cannabinoid ligands to investigate the functionality of plasmalemmal versus intracellular CB_2 receptors in U2OS cells stably expressing CB_2.

EXPERIMENTAL PROCEDURES

Chemicals. Anandamide, AM630, WIN55,212-2, 2-arachidonoyl glycerol (2-AG), and D-[Trp7,9,10]-substance P were obtained from Tocris Bioscience (R&D Systems, Minneapolis, MN). All other chemicals were from Sigma (St. Louis, MO).

Cell Culture. The CB_2-β-arrestin2-GFP-U2OS (CB_2-U2OS) cell line was kindly provided by M. Caron and L. S. Barak (Duke University, Durham, NC); the CB_2 receptor sequence is the CNR2_Human sequence (GenBank accession code P34972). CB_2-U2OS cells were maintained in DMEM supplemented with 10% fetal bovine serum, 100 mg/mL

Received: May 23, 2014
Revised: July 13, 2014
Published: July 17, 2014

   dx.doi.org/10.1021/bi500632a | Biochemistry 2014, 53, 4990−4999

Zeocin, and 200 μg/mL G418 at 37 °C in a humidified incubator with 5% CO_2. The serum was removed 24 h prior to experimentation. In experiments that aimed to evaluate Gq-dependent signaling, cell starvation was concomitant with incubation of D-[Trp7,9,10]-substance P (24 h).

Immunocytochemistry and Confocal Imaging Studies. U2OS cells transiently transfected with the GFP-tagged CB_2 receptor (kindly provided by M. Caron and L. S. Barak) and with Rab7-RFP (Addgene, Cambridge, MA) 48 h earlier were fixed with 4% paraformaldehyde, washed in phosphate-buffered saline, and mounted with DAPI Fluoromont G (Southern Biotech, Birmingham, AL). Cells were imaged using a Carl Zeiss 710 two-photon confocal microscope with a 63× oil immersion objective, using a 1× digital zoom, with excitations set for DAPI, GFP, and DsRed at 405, 488, and 561 nm, respectively. Images were analyzed using Zen 2010 (Zeiss), as previously reported.[16]

Calcium Imaging. Measurements of $[Ca^{2+}]_i$ were performed as previously described.[16−19] Briefly, cells were incubated with 5 μM Fura-2 AM (Invitrogen) in HBSS at room temperature for 45 min, washed with dye-free HBSS, and incubated for an additional 45 min to allow dye de-esterification. Coverslips were mounted in an open bath chamber (RP-40LP, Warner Instruments, Hamden, CT) on the stage of an inverted microscope (Nikon Eclipse TiE, Nikon Inc., Melville, NY), equipped with a Perfect Focus System and a Photometrics CoolSnap HQ2 CCD camera (Photometrics, Tucson, AZ). During the experiments, the Perfect Focus System was activated. Fura-2 AM fluorescence (emission at 510 nm), following alternate excitation at 340 and 380 nm, was acquired at a frequency of 0.25 Hz. Images were acquired and analyzed using NIS-Elements AR version 3.1 (Nikon Inc.). After appropriate calibration with ionomycin and $CaCl_2$, and Ca^{2+}-free and EGTA, respectively, the ratio of the fluorescence signals (340 nm to 380 nm) was converted to Ca^{2+} concentration.[20]

Intracellular Microinjection. Injections were performed using Femtotips II, InjectMan NI2, and FemtoJet systems (Eppendorf) as previously reported.[16−19] Pipettes were back-filled with an intracellular solution containing 110 mM KCl, 10 mM NaCl, and 20 mM HEPES (pH 7.2) or the compounds to be tested. The injection time was 0.4 s at 60 hectoPascal with a compensation pressure of 20 hectoPascal to ensure that the microinjected volume was <1% of the cell volume. The intracellular concentration of chemicals was determined on the basis of the concentration in the pipet and the volume of injection. The cells to be injected were Z-scanned before injection, and the cellular volume was automatically calculated by NIS-Elements AR version 3.1 (Nikon Inc.).

Statistics. Data are expressed as means and the standard error of the mean. One-way analysis of variance, followed by post hoc Bonferroni and Tukey tests, was used to assess significant differences between groups; $P < 0.05$ was considered statistically significant.

RESULTS

Effects of Extracellular versus Intracellular Administration of CB_2 Agonist 2-Arachidonoyl Glycerol on the Cytosolic Ca^{2+} Concentration of CB_2-Expressing U2OS Cells. We evaluated the Ca^{2+} response of U2OS cells stably expressing the CB_2 receptor to bath application and intracellular microinjection of the endocannabinoid 2-arachidonoyl glycerol (2-AG). Increasing concentrations of 2-AG (0.01, 0.1, and 1 μM) were applied extracellularly to CB_2-U2OS cells, which elevated the intracellular Ca^{2+} concentration, $[Ca^{2+}]_i$, by 7 ± 3.4 nM (n = 31 cells), 12 ± 5.1 nM (n = 43 cells), and 87 ± 3.1 nM (n = 56 cells), respectively (Figure 1A). The effect of

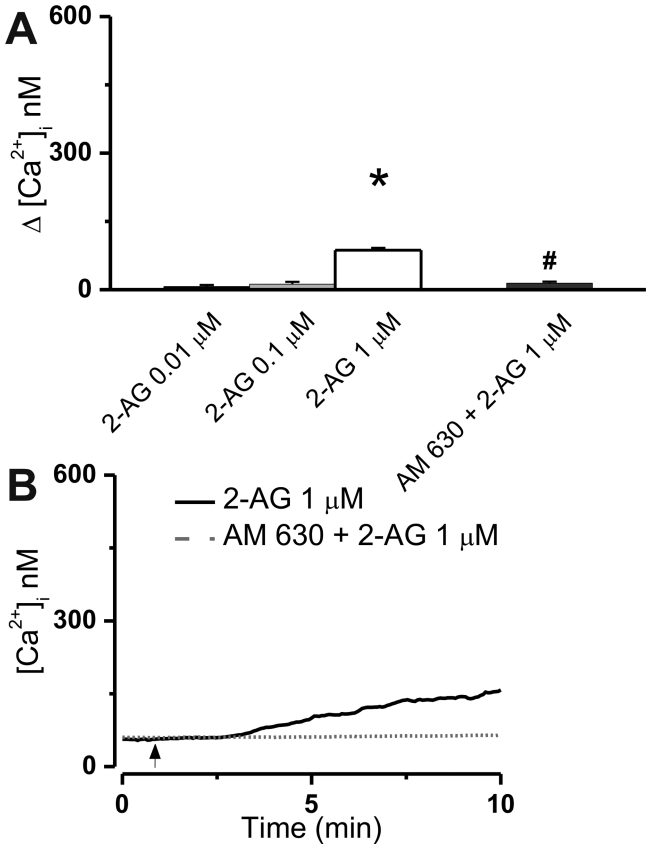

Figure 1. Extracellular administration of 2-arachidonoyl glycerol (2-AG) to CB_2-U2OS cells elevates $[Ca^{2+}]_i$. (A) Comparison of the increases in $[Ca^{2+}]_i$ produced by extracellular administration of 2-AG (0.01−1 μM) and 1 μM 2-AG in the presence of CB_2 receptor antagonist AM630 (1 μM); $P < 0.05$ compared with basal levels (*) or with 1 μM 2-AG (#). (B) Representative recordings of increases in $[Ca^{2+}]_i$ in response to 1 μM 2-AG in absence or presence of 1 μM CB_2 antagonist AM630.

the latter concentration of 2-AG was statistically significant ($P < 0.05$) and sensitive to CB_2 blockade with AM630 (1 μM, 10 min). In the presence of AM630, $\Delta[Ca^{2+}]_i$ was reduced to 14 ± 3.6 nM (n = 49) (Figure 1A,B). The effect of 2-AG on $[Ca^{2+}]_i$ was delayed by 1−2 min and increased gradually (Figure 1B).

In experiments using the intracellular microinjection technique, injection of 0.01, 0.1, and 1 μM 2-AG (final concentrations inside the cell) induced robust and significant increases in $[Ca^{2+}]_i$ of CB_2-U2OS cells of 264 ± 11 nM (n = 6 cells), 653 ± 19 nM (n = 6 cells), and 938 ± 22 nM (n = 6 cells), respectively, while control buffer microinjection had an insignificant effect of 49 ± 4 nM (n = 6 cells) (Figure 2A−D). In the presence of co-injected CB_2 antagonist AM630 (1 μM), 0.1 μM 2-AG elevated $[Ca^{2+}]_i$ by 58 ± 4 nM (n = 6 cells), similar to that of control buffer microinjection; the effect of 0.1 μM 2-AG on $[Ca^{2+}]_i$ of untransfected U2OS cells was also insignificant, measuring 34 ± 5 nM (n = 6 cells) (Figure 2A,B,E,F).

In all series of experiments using intracellular injection, CB_2-U2OS cells were pretreated for 1 min with 1 μM AM630

dx.doi.org/10.1021/bi500632a | Biochemistry 2014, 53, 4990−4999

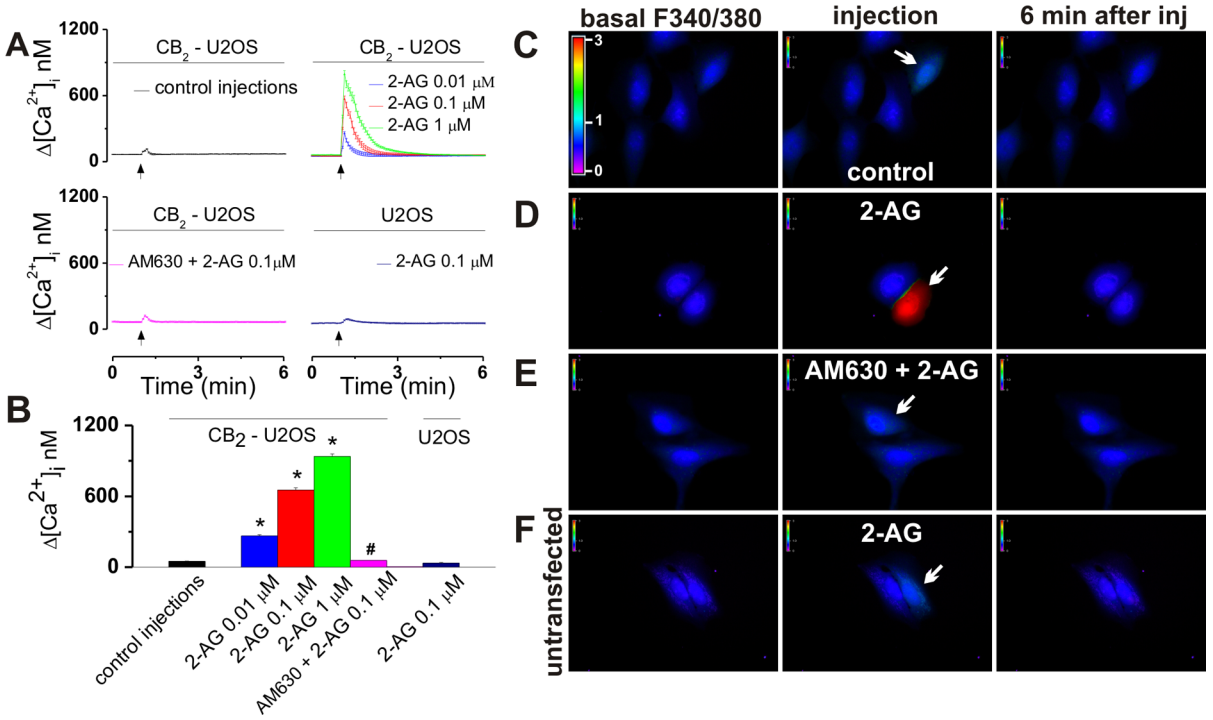

Figure 2. Intracellular microinjection of 2-AG into CB_2-U2OS cells produces CB_2-dependent Ca^{2+} elevation. (A) Averaged increases in $[Ca^{2+}]_i$ produced by intracellular administration of control buffer (top left) or 2-AG (0.01, 0.1, and 1 μM, final concentrations inside the cell, top right), co-injection of 0.1 μM 2-AG with CB_2 antagonist AM630 (1 μM, bottom left) in CB_2-U2OS cells, or microinjection of 0.1 μM 2-AG into control U2OS cells (bottom right). (B) Comparison of the Ca^{2+} responses elicited by the treatments of CB_2-U2OS or control untransfected U2OS cells mentioned above; $P < 0.05$ when compared with the control (*) or with 2-AG alone (#). (C–F) Characteristic fluorescence images of Fura-2 AM-loaded CB_2-U2OS cells before (left), during (middle), and 6 min after (right) intracellular administration of control buffer (C), 0.1 μM 2-AG alone (D), or 0.1 μM 2-AG in the presence of 1 μM AM630 (E) or of U2OS cells treated with 0.1 μM 2-AG (F). Arrows denote the injected cells; the fluorescence scale (0–3) is illustrated in each panel and magnified in the left panel of part C.

(applied extracellularly), to exclude the possibility that the injected cannabinoid ligands leaked from the pipet and triggered plasma membrane receptor-mediated effects.

Functional and Morphological Evidence of Localization of CB_2 to Endolysosomes in CB_2-Transfected U2OS Cells. CB_2-U2OS cells were incubated for 1 h with either 1 μM bafilomycin A1, a V-type ATPase that prevents lysosomal acidification,[21] or 30 μM rapamycin, which blocks the last step of the engulfment of molecules by endolysosomes via microautophagy.[22] Under the conditions described above, the effect of 0.1 μM 2-AG on $[Ca^{2+}]_i$, initially measuring 653 ± 19 nM, was drastically reduced to 36 ± 4.8 nM (n = 6 cells) and 67 ± 9.1 nM (n = 6 cells) (Figure 3A–E). In U2OS cells co-expressing GFP-tagged CB_2 receptors and RFP-tagged Rab7, a small GTPase associated with both endosomes and lysosomes,[23] we observed an extensive colocalization of CB_2 and Rab7 (Figure 3F). Lysosomal disruption using bafilomycin A1 greatly reduced the extent of the merged signal of CB_2 and Rab7 (Figure 3F).

Intracellular, but Not Extracellular, Administration of Anandamide Elevates the Cytosolic Ca^{2+} Concentration of CB_2-Expressing U2OS Cells. CB_2-U2OS cells extracellularly treated with progressive concentrations of anandamide (0.01, 0.1, and 1 μM) failed to respond with a significant increase in $[Ca^{2+}]_i$ (Figure 1 of the Supporting Information); incubation with CB_2 antagonist AM630 (1 μM) did not modify the response to 1 μM anandamide (Figure 1 of the Supporting Information).

However, CB_2-U2OS cells responded to intracellular administration of anandamide (0.01, 0.1, and 1 μM, final concentrations inside the cell) with significant and concentration-dependent elevations of $[Ca^{2+}]_i$: 124 ± 7.4, 368 ± 8.4, and 574 ± 7.2 nM, respectively [n = 6 cells for each concentration tested (Figure 4A,B)]. The anandamide-induced increase in $[Ca^{2+}]_i$ was fast and transient (Figure 4A); blockade of intracellular CB_2 receptors upon co-injection of 1 μM AM630 prevented the effect of microinjected anandamide (1 μM), reducing it to 37 ± 4.1 nM [n = 6 cells (Figure 4A–D)], a response similar to that elicited by control buffer microinjection (Figure 2). Characteristic images depicting the increases in the Fura-2 fluorescence ratio at 340 and 380 nm upon microinjection of anandamide (1 μM) in the absence or presence of AM630 (1 μM) are shown in panels C and D of Figure 4.

Anandamide produced negligible effects in control untransfected U2OS cells regardless of whether it was applied extracellularly (Figure 2 of the Supporting Information) or intracellularly (Figure 3 of the Supporting Information).

WIN55,212-2 Produces CB_2 Receptor-Dependent Increases in Ca^{2+} Concentration in CB_2-U2OS Cells. Extracellular administration of WIN55,212-2 (0.01, 0.1, and 1 μM) elevated $[Ca^{2+}]_i$ by 11 ± 8.1 nM (n = 27 cells), 17 ± 6.3 nM (n = 38 cells), and 262 ± 6.8 nM [n = 46 cells (Figure 5A,B)]; the latter effect was statistically significant ($P < 0.05$) and sensitive to CB_2 blockade with AM630 [1 μM, incubation for 10 min, $\Delta[Ca^{2+}]_i$ reduced to 12 ± 6.8 nM (n = 36 cells)] (Figure 5A,B). The Ca^{2+} response elicited by WIN55,212-2

dx.doi.org/10.1021/bi500632a | Biochemistry 2014, 53, 4990–4999

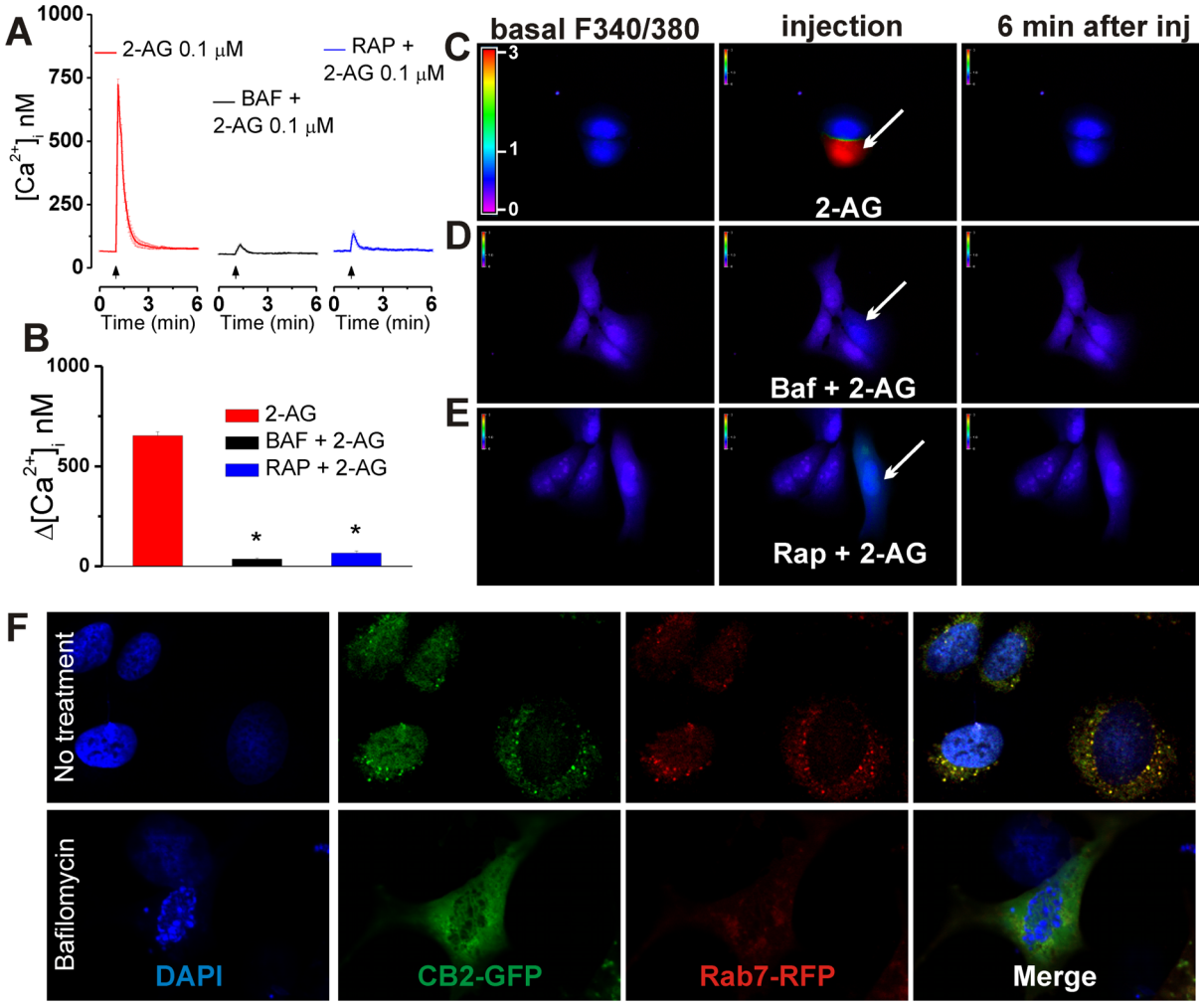

Figure 3. Intracellular CB_2 receptors are located at endolysosomes in CB_2-expressing U2OS cells. (A) Averaged Ca^{2+} responses of CB_2-U2OS cells to intracellular administration of 0.1 μM 2-AG in the absence (left) or presence of lysosomal disruptor bafilomycin A1 (1 μM, incubation for 1 h, middle) or microautophagy inhibitor rapamycin (30 μM, incubation for 1 h, right). (B) Comparison of the increases in $[Ca^{2+}]_i$ elicited by 2-AG under the conditions described above; $P < 0.05$ when compared with 2-AG microinjection (*). (C–E) Representative fluorescence images of Fura-2 AM-loaded CB_2-U2OS cells before (left), during (middle), and 6 min after (right) intracellular administration of 0.1 μM 2-AG in the absence (C) and presence of bafilomycin A1 (D) or rapamycin (E). (F) Confocal images (top row) showing the colocalization of the GFP-tagged CB_2 receptor and RFP-tagged Rab7, an endolysosomal marker, in GFP-CB_2- and RFP-Rab7-transfected U2OS cells; the nuclei are labeled with DAPI (blue). Lysosomal disruption (bottom row) with bafilomycin A1 markedly reduces the extent of the merged immunostaining of CB_2 and Rab7.

occurred with a latency of 1–2 min (Figure 5B), similar to the effect of bath-applied 2-AG (Figure 1B).

Microinjection of WIN55,212-2 (0.01, 0.1, and 1 μM, final concentrations inside the cell) into CB_2-U2OS cells triggered fast, transient, and concentration-dependent increases in $[Ca^{2+}]_i$ of 257 ± 5.3, 635 ± 7.1, and 924 ± 17 nM (n = 6 cells for each concentration tested), whereas when 1 μM AM630 was co-injected with 1 μM WIN55,212-2, a small and insignificant increase in Ca^{2+} concentration, of 31 ± 4.6 nM (n = 6 cells), was apparent (Figure 6A,B). Representative examples of the increase in the F_{340}/F_{380} fluorescence ratio produced by intracellular administration of WIN55,212-2 or AM630 and WIN55,212-2 are shown in panels C and D of Figure 6. The insignificant Ca^{2+} responses to extracellular and intracellular administration of WIN55,212-2 in control U2OS cells are illustrated in Figures 2 and 3 of the Supporting Information, respectively.

Effects of Extracellular 2-AG and WIN55,212-2 Are Mediated by Gq Coupling of CB_2 Receptors. 2-AG (1 μM), anandamide (1 μM), or WIN55,212-2 (1 μM) was bath-applied to CB_2-U2OS cells treated overnight with chemicals interfering with G protein signaling. After cholera toxin (CTX, 100 ng/mL) pretreatment, 2-AG produced an increase in the $[Ca^{2+}]_i$ of 83 ± 5.1 nM [n = 61 cells (Figure 7A,B)] similar to the effect of 2-AG on untreated cells. CTX irreversibly abolishes the GTPase activity of the Gs α subunit, inducing continual activation of adenylyl cyclase and increased intracellular levels of cAMP. In this manner, it hinders ligands of Gs-coupled receptors from eliciting their Gs-dependent effects. After pretreatment with the Gi/o inhibitor pertussis toxin (PTX, 100 ng/mL), the response of 2-AG was negligibly modified, measuring 85 ± 4.2 nM [n = 53 cells (Figure 7A,B)]. Conversely, pretreatment of CB_2-U2OS cells with Gq blocker D-[Trp7,9,10]-substance P (D-SP, 100 ng/mL)[24] greatly reduced the effect of 2-AG to 7 ± 2.7 nM [n = 67 cells (Figure 7A,B)].

The Ca^{2+} response elicited by anandamide was largely similar and not significant regardless of whether anandamide was

dx.doi.org/10.1021/bi500632a | Biochemistry 2014, 53, 4990–4999

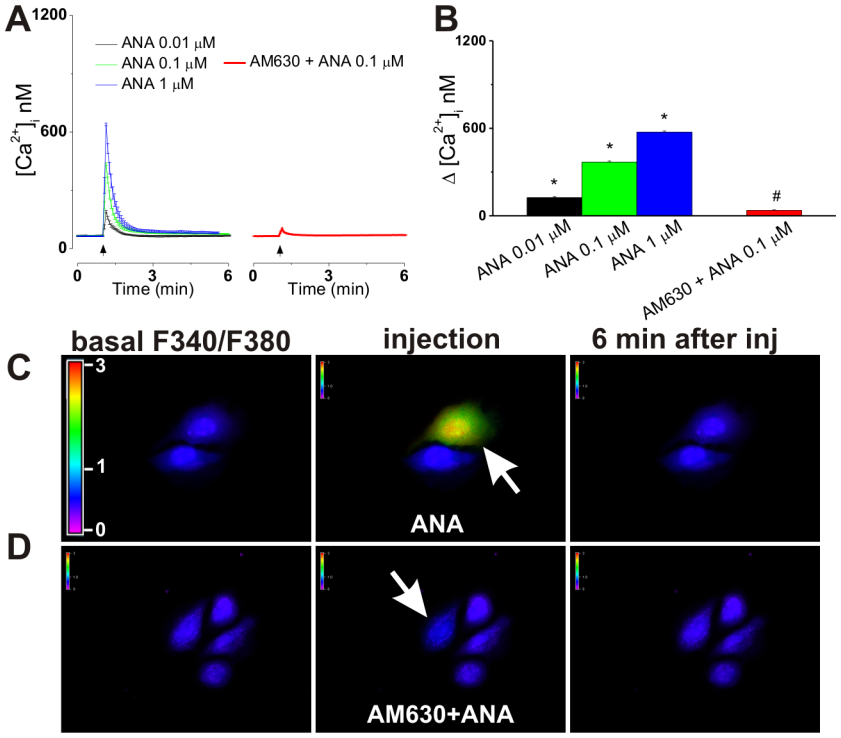

Figure 4. Intracellular administration of anandamide increases $[Ca^{2+}]_i$ in CB_2-U2OS cells. (A) Averaged Ca^{2+} responses induced by increasing doses of microinjected anandamide (ANA, 0.01−1 μM, left) or by co-injection of 0.1 μM anandamide and 1 μM CB_2 antagonist AM630 (right). (B) Comparison of the increases in $[Ca^{2+}]_i$ produced by microinjected anandamide (0.01, 0.1, and 1 μM) and anandamide (0.1 μM) in the presence of AM630 (1 μM); $P < 0.05$ compared with the control (∗) (see Figure 2) or with 0.1 μM anandamide alone (#). (C and D) Typical fluorescence images of Fura-2 AM-loaded CB_2-U2OS cells before (left), during (middle), and 6 min after (right) intracellular administration of 0.1 μM anandamide alone (C) or in the presence of 1 μM AM630 (D). Arrows denote the injected cells; the fluorescence scale (0−3) is illustrated in each panel and magnified in the left panel of part C.

applied alone [$\Delta[Ca^{2+}]_i$ of 9 ± 4.7 nM (n = 33 cells)] or after stimulating Gs-dependent signaling with CTX (100 ng/mL), inhibiting Gi/o with PTX (100 ng/mL), and inhibiting Gq with D-SP (100 ng/mL). The $\Delta[Ca^{2+}]_i$ values were 8 ± 5.2 nM (n = 29 cells), 6 ± 4.8 nM (n = 41 cells), and 7 ± 2.3 nM (n = 36 cells), respectively (Figure 7A,B).

D-SP pretreatment drastically diminished the effect induced by WIN55,212-2, reducing it to 58 ± 3.9 nM, while in the presence of CTX or PTX, WIN55,212-2 increased $[Ca^{2+}]_i$ to similar extents as in their absence: $\Delta[Ca^{2+}]_i$ values were 257 ± 6.8 nM (n = 53 cells) and 243 ± 7.9 nM (n = 47 cells) in cells pretreated with CTX and PTX, respectively, and 262 ± 6.8 nM (n = 49 cells) for WIN55,212-2 alone (Figure 7A,B).

Intracellular CB_2 Receptors Couple to Gq Proteins. Overnight treatment of CB_2-U2OS cells with CTX (100 ng/mL) or PTX (100 ng/mL) failed to significantly modify the Ca^{2+} response elicited by intracellular administration of 0.1 μM 2-AG (Figure 8A,B). Under the conditions described above, 2-AG increased $[Ca^{2+}]_i$ by 654 ± 21 nM (n = 6 cells) and 629 ± 18 nM (n = 6 cells), respectively, while the response to 2-AG alone measured 652 ± 19 nM [n = 6 cells (Figure 8A,B)]. After incubation of cells with D-SP (100 ng/mL), the effect of 2-AG was greatly decreased to 62 ± 23 nM (n = 6 cells), indicating participation of a Gq-dependent pathway in the response (Figure 8A,B).

Upon pretreatment with CTX (100 ng/mL) or PTX (100 ng/mL), intracellular injection of anandamide (0.1 μM) elevated $[Ca^{2+}]_i$ of CB_2-U2OS cells by 359 ± 7.2 nM (n = 6 cells) or 355 ± 11.2 nM (n = 6 cells), respectively; these effects are similar to those triggered by microinjected anandamide alone [368 ± 8.4 nM (n = 6 cells)], indicating that Gs and Gi/o proteins are not mediating its effect. Upon D-SP (100 ng/mL) pretreatment, intracellular anandamide produced an insignificant Ca^{2+} response of 38 ± 6.3 nM [n = 6 cells (Figure 8A,B)].

Similarly, CTX and PTX (both at 100 ng/mL) pretreatment did not significantly modify the response of CB_2-U2OS cells to microinjected WIN55,212-2 (0.1 μM). $\Delta[Ca^{2+}]_i$ values were 668 ± 13 nM (n = 6 cells) and 641 ± 9.8 nM (n = 6 cells) after CTX and after PTX, respectively, and 635 ± 7.1 nM for WIN55,212-2 alone. However, blocking Gq proteins with 100 ng/mL D-SP basically abolished the effect of intracellular WIN55,212-2. In this case, $\Delta[Ca^{2+}]_i$ decreased to 27 ± 5.4 nM [n = 6 cells (Figure 8A,B)].

Activation of Intracellular CB_2 Mobilizes Ca^{2+} from Distinct Pools. CB_2-U2OS cells incubated with Ca^{2+}-free saline responded to microinjection of 0.1 μM 2-AG with a 457 ± 5.2 nM increase in $[Ca^{2+}]_i$ (n = 6 cells), while the effect of control buffer microinjection was negligible {$\Delta[Ca^{2+}]_i$ = 29 ± 1.7 nM [n = 6 cells (Figure 9A,B)]}. The response to 2-AG was reduced in Ca^{2+}-free versus Ca^{2+}-containing HBSS [$\Delta[Ca^{2+}]_i$ = 653 ± 19 nM (Figure 2)], indicating mobilization of both intracellular and extracellular Ca^{2+} pools. Using a pharmacological approach, we further sought to identify the intracellular sources of Ca^{2+} involved in the response to microinjected 2-AG. Pretreatment of cells with ryanodine receptor blocker ryanodine (10 μM, 1 h) did not significantly modify the Ca^{2+} response to 2-AG, which measured 452 ± 5.9 nM [n = 6 cells (Figure 9A,B)]. Conversely, pretreatment with Ned-19 (5 μM, 15 min), which blocks endolysosomal Ca^{2+} release via the NAADP-sensitive two-pore channels,[25] decreased the extent of

dx.doi.org/10.1021/bi500632a | Biochemistry 2014, 53, 4990−4999

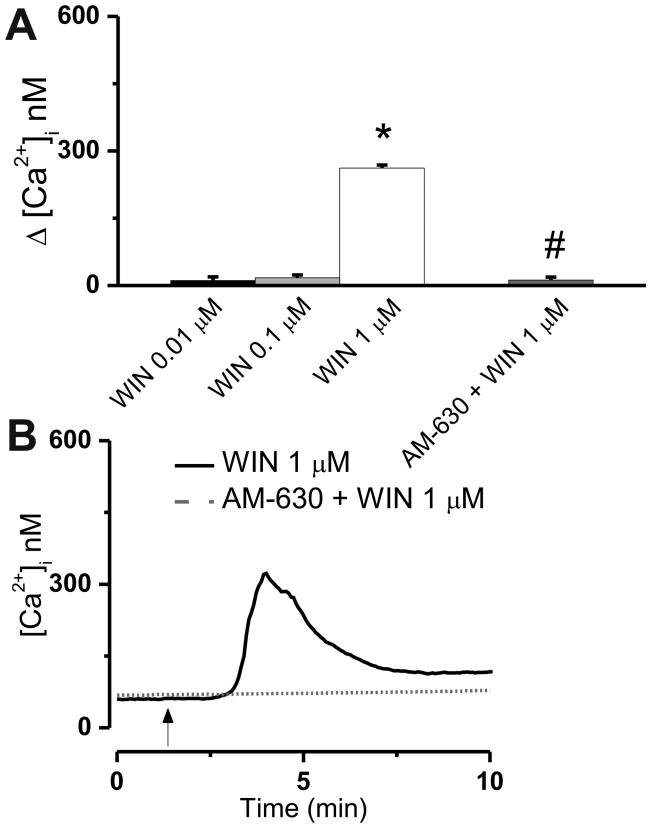

Figure 5. Extracellular administration of WIN55,212-2 to CB_2-U2OS cells elevates $[Ca^{2+}]_i$. (A) Comparison of the increases in $[Ca^{2+}]_i$ produced by extracellular administration of WIN55,212-2 (WIN, 0.01−1 μM) and 1 μM WIN55,212-2 in the presence of CB_2 receptor antagonist AM630 (1 μM); $P < 0.05$ compared with basal levels (*) or with 1 μM WIN55,212-2 (#). (B) Representative recordings of increases in $[Ca^{2+}]_i$ in response to 1 μM WIN in the absence or presence of 1 μM CB_2 antagonist AM630.

the Ca^{2+} elevation produced by 2-AG to 349 ± 4.3 nM (n = 6 cells); inositol 1,4,5-trisphosphate receptor (IP_3R) inhibition induced by treating CB_2-U2OS cells with heparin and xestospongin C (10 μM, 15 min) also induced a significant decrease in the response to 2-AG {$\Delta[Ca^{2+}]_i$ = 168 ± 3.6 nM [n = 6 cells (Figure 9A,B)]}. When both IP_3Rs and the two-pore channels were blocked, the Ca^{2+} response to intracellular microinjection of 2-AG was completely abolished {$\Delta[Ca^{2+}]_i$ = 34 ± 2.4 nM [n = 6 cells (Figure 9A,B)]}.

DISCUSSION

In addition to the effects initiated at the plasma membrane, G protein-coupled receptors (GPCRs) may also trigger signaling cascades upon their activation within the cell.[26] The emerging paradigm of functional intracellular GPCRs is particularly significant in the case of lipid messengers that are generated intracellularly and may target their receptors at both sites, (reviewed in ref 27). We and others reported the functionality of intracellularly expressed CB_1 receptors,[17,28] as well as their ability to use Ca^{2+} as a second messenger.[17] To evaluate whether CB_2 receptors elicit Ca^{2+} signaling upon plasmalemmal or intracellular activation, cannabinoid ligands were administered extracellularly or microinjected into U2OS cells stably expressing CB_2.

We noticed that extracellular administration of 2-AG induced a small increase in $[Ca^{2+}]_i$ of CB_2-U2OS cells only at the highest concentration tested here (1 μM). Bath application of anandamide did not elevate $[Ca^{2+}]_i$ of CB_2-U2OS cells. While 2-AG produced a gradual increase in $[Ca^{2+}]_i$ of CB_2-U2OS cells, a robust Ca^{2+} response was induced by extracellular administration of WIN55,212-2, which is a cannabinoid agonist displaying high affinity and/or intrinsic activity at this receptor.[1,29] The CB_2 specificity was indicated by the ability of CB_2 antagonist AM630[29] to inhibit the effects of extracellular administration of 2-AG and WIN55,212-2 in CB_2-U2OS cells and by the unresponsiveness of untransfected U2OS cells to bath application of WIN55,212-2.

Similar to CB_1, CB_2 receptors couple to Gi proteins and inhibit cAMP formation or activate MAPK.[6,29] However, coupling to Gs or Gq of CB_1 receptors has also been reported.[30,31] While a cannabinoid-dependent $[Ca^{2+}]_i$ increase may occur downstream of Gi,[32,33] we noticed that the CB_2-dependent effects of 2-AG or WIN55,212-2 were completely contingent on Gq in our paradigm. WIN55,212-2 also activates Gq downstream of CB_1;[31] moreover, it can trigger a CB_2-dependent signaling pathway different from that elicited by other ligands.[7] Thus, the discrepancy between the effects of extracellular administration of anandamide, 2-AG, and WIN55,212-2 in our study may be a result of the reported functional selectivity at CB_2 receptors.[7,34]

In a recent study, we demonstrated that anandamide can trigger fast CB_1-dependent Ca^{2+} signaling upon microinjection but is ineffective upon extracellular administration in CB_1-transfected cells.[17] To test the hypothesis of functional intracellular CB_2 receptors in CB_2-U2OS cells, intracellular injections of 2-AG, anandamide, or WIN55,212-2 were conducted. When 2-AG or anandamide was microinjected, concentration-dependent elevations of $[Ca^{2+}]_i$ were observed, and the Ca^{2+} response pattern was very fast, which is in contrast with the delayed, modest response and lack of effect, respectively, observed with the extracellular administration of these two agonists. Likewise, intracellular administration of WIN55,212-2 resulted in a concentration-dependent and robust effect. WIN55,212-2 and 2-AG produced Ca^{2+} responses with an amplitude higher than that of anandamide, which is consistent with the full agonistic activity at CB_2 receptors reported for these ligands.[1,29] The sensitivity of these responses to the intracellular blockade of CB_2 and the unresponsiveness of control, untransfected U2OS cells to microinjected cannabinoids were considered to be indicative of CB_2 specificity. We further noticed that interfering with Gq-dependent, but not with Gs- or Gi/o-dependent, signaling prevented the effect of microinjected 2-AG, anandamide, or WIN55,212-2. Moreover, the endocannabinoids and WIN55,212-2 trigger similar signaling pathways upon intracellular administration, despite their unrelated chemical structure.

The accumulating evidence pointing to endolysosomes as intracellular locations where GPCRs initiate signaling[16,18,19,35,36] prompted us to evaluate whether this may be the case for CB_2. In an initial functional study, we found that the effect of intracellular 2-AG is abolished by lysosomal disruption. Because rapamycin reduced the effects of microinjected 2-AG, ligand microautophagy[22] may be a necessary step in the activation of endolysosomally located CB_2. The localization of CB_2 to lysosomes was confirmed by an additional study, providing morphological evidence that CB_2 colocalizes with the endolysosomal-associated small GTPase Rab7. Lysosomal disruption with bafilomycin A1 markedly

dx.doi.org/10.1021/bi500632a | Biochemistry 2014, 53, 4990−4999

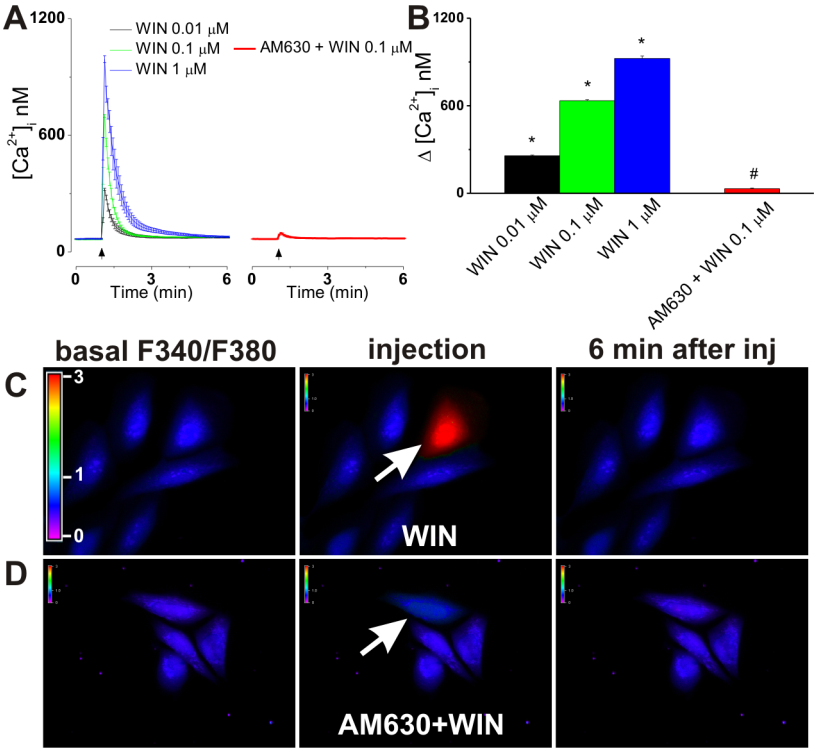

Figure 6. Microinjection of WIN55,212-2 increases $[Ca^{2+}]_i$ in CB_2-U2OS cells. (A) Averaged $[Ca^{2+}]_i$ elevations produced by increasing doses of microinjected WIN55,212-2 (WIN 0.01−1 μM, left) or by co-injection of 0.1 μM WIN55,212-2 and 1 μM CB_2 antagonist AM630 (right). (B) Comparison of the increases in $[Ca^{2+}]_i$ elicited by microinjected WIN55,212-2 (0.01, 0.1, and 1 μM) and WIN55,212-2 (0.1 μM) in the presence of AM630 (1 μM); $P < 0.05$ compared with the control (∗) (see Figure 2) or with 0.1 μM WIN55,212-2 alone (#). (C and D) Characteristic fluorescence images of Fura-2 AM-loaded CB_2-U2OS cells before (left), during (middle), and 6 min after (right) intracellular administration of 0.1 μM WIN55,212-2 alone (C) or in the presence of 1 μM AM630 (D). Arrows denote the injected cells; the fluorescence scale (0−3) is illustrated in each panel and magnified in the left panel of part C.

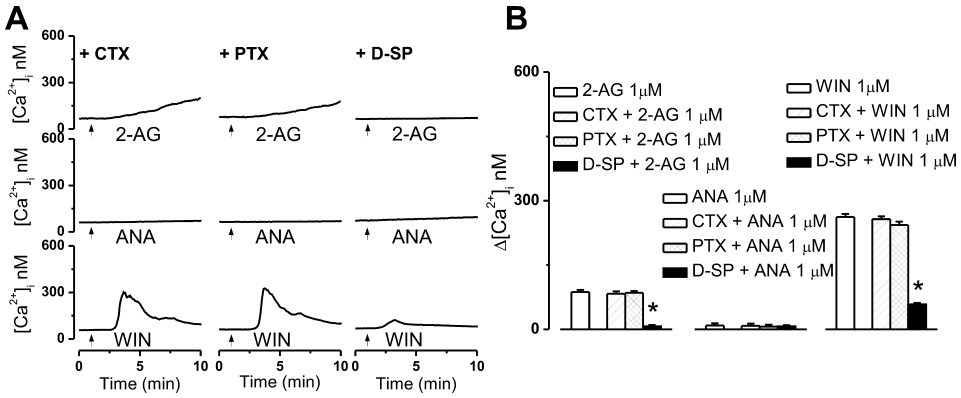

Figure 7. The Ca^{2+} responses produced by bath-applied 2-AG and WIN55,212-2 are prevented by a Gq protein inhibitor. (A) Representative examples of the Ca^{2+} responses induced by 1 μM 2-AG (top), 1 μM anandamide (ANA, middle), or 1 μM WIN55,212-2 (WIN, bottom), applied by bath to CB_2-expressing U2OS cells in the presence of cholera toxin (CTX, 100 nM, top), which occludes Gs-dependent signaling, Gi/o blocker pertussis toxin (PTX, 100 nM, middle), or Gq protein inhibitor D-[Trp7,9,10]-substance P (D-SP, 100 μM, bottom); 2-AG and WIN55,212-2 increased $[Ca^{2+}]_i$, and the response was Gq protein-mediated. (B) Comparison of the mean amplitude of the Ca^{2+} responses produced by extracellular administration of 1 μM 2-AG (left), 1 μM anandamide (middle), or 1 μM WIN55,212-2 (right) in the absence and presence of the indicated G protein inhibitors; $P < 0.05$ compared with WIN55,212-2 alone (∗).

reduced the fluorescence intensity of both CB_2 and Rab7, supporting the findings of the functional study.

Next, we sought to examine the pools of Ca^{2+} mobilized upon activation of intracellularly located CB_2. The reduction in the amplitude of the Ca^{2+} response of CB_2-U2OS cells incubated with Ca^{2+}-free saline to microinjected 2-AG indicated that both influx of extracellular Ca^{2+} and release of Ca^{2+} from intracellular stores occur downstream of intracellular CB_2 activation. Using a pharmacological approach, we further determined that 2-AG-induced stimulation of intracellular CB_2 results in Ca^{2+} mobilization from endolysosomes via NAADP-sensitive two-pore channels and from the endoplasmic reticulum via the IP_3R. This effect correlates well with the localization of CB_2 at the endolysosmes, as well as with the localization of NAADP-generating enzymes[37,38] at the membrane of acidic organelles.[39]

dx.doi.org/10.1021/bi500632a | *Biochemistry* 2014, 53, 4990−4999

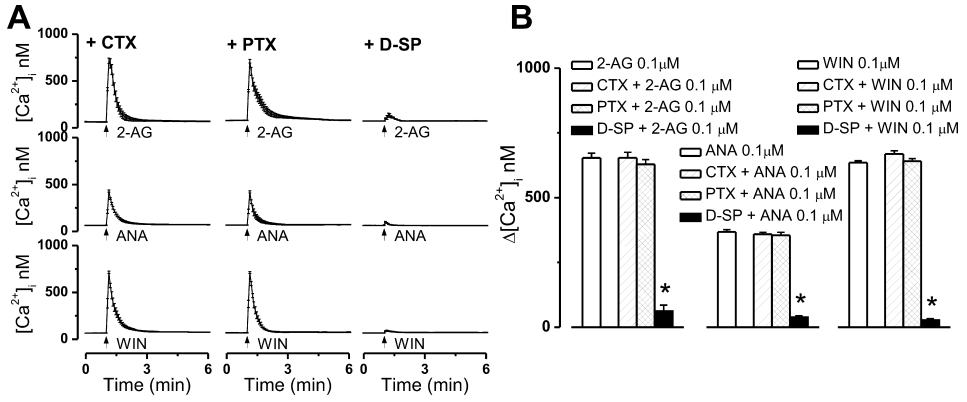

Figure 8. Intracellular microinjection of 2-AG, anandamide, or WIN55,212-2 produces Gq-dependent Ca^{2+} responses in CB_2-expressing U2OS cells. (A) Averaged Ca^{2+} responses induced by intracellular administration of 0.1 μM 2-AG (top), 0.1 μM anandamide (ANA, middle), or 0.1 μM WIN55,212-2 (WIN, bottom) in CB_2-U2OS cells pretreated with cholera toxin (CTX, 100 nM, top), pertussis toxin (PTX, 100 nM, middle), or Gq protein inhibitor D-[Trp7,9,10]-substance P (D-SP, 100 μM, bottom); each ligand increased $[Ca^{2+}]_i$, and the response was sensitive to Gq protein blockade. (B) Comparison of the mean amplitude of the Ca^{2+} responses produced by intracellular administration of 0.1 μM 2-AG (left), 0.1 μM anandamide (middle), or 0.1 μM WIN55,212-2 (right) in absence and presence of the indicated G protein inhibitors; in each group of data, $P < 0.05$ compared with 2-AG, anandamide, or WIN55,212-2 alone (∗).

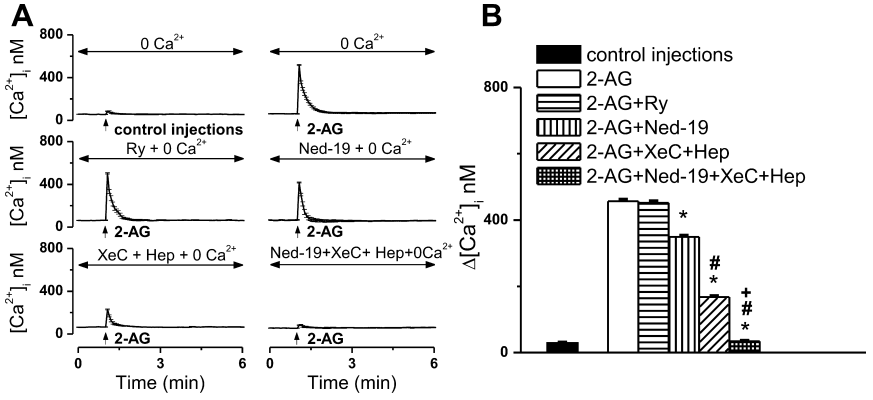

Figure 9. 2-AG mobilizes endoplasmic reticulum and acidic-like Ca^{2+} stores. (A) Averaged Ca^{2+} responses of CB_2-U2OS cells in Ca^{2+}-free saline, microinjected with either control buffer or 0.1 μM 2-AG in the absence or presence of ryanodine receptor blocker ryanodine (Ry), two-pore channel antagonist Ned-19, IP_3R inhibitors xestospongin C (XeC) and heparin (Hep), or a combination of Ned-19, XeC, and Hep. (B) Comparison of the Ca^{2+} increases produced by the treatments described in (A); $P < 0.05$ compared with 2-AG microinjection (∗), 2-AG in the presence of Ned-19 (#), or 2-AG in the presence of IP_3R blockers (+).

Thus, we conclude that intracellular CB_2 receptors are functional, endolysosomally located, and Gq-coupled in CB_2-U2OS cells, and their activation mobilizes NAADP-sensitive acidic-like Ca^{2+} stores and inositol 1,4,5-trisphosphate-sensitive endoplasmic reticulum pools. In addition, we note that CB_2 agonists elicit discrepant and delayed effects and exhibit a considerably lower potency when administered extracellularly as opposed to intracellularly. Although these effects appear to be Gq-mediated, it may be that a considerable pool of plasmalemmal CB_2 receptors do not couple with Gq/Ca^{2+} signaling. Conversely, Gq coupling and associated Ca^{2+} responses may be a characteristic of intracellularly located CB_2, in which case the delay in the effects elicited by agonists upon extracellular administration may be a result of the latency necessary for membrane permeation. Nonetheless, differential activation of plasmalemmal CB_2 by the three agonists (applied extracellularly) is more likely to be a result of the functional selectivity at CB_2,[7,34] which is supported by the previous finding that 2-AG (which promotes agonist-directed trafficking at CB_2[34]) has a low potency at eliciting CB_2-mediated Ca^{2+} responses.[34] Binding of a particular agonist to a GPCR results in the enrichment of a unique set of receptor conformations based on the microaffinity of the agonist for each conformation; because distinct conformations presumably couple receptors differently to specific G proteins and intracellular effectors, individual agonists ultimately produce distinct effects.[11] As such, anandamide, 2-AG, and WIN55,212-2 may induce conformational changes in plasmalemmal CB_2, resulting in distinct responses, as observed in the study presented here. However, we note that this is not the case with intracellular, endolysosomally located CB_2, which appears to couple to the same Gq-mediated Ca^{2+} pathway in response to intracellular administration of the three agonists; moreover, the three agonists have higher potency and efficacy at eliciting intracellularly initiated CB_2-dependent Ca^{2+} responses. Thus, functional selectivity may apply more to plasmalemmal than to intracellular CB_2.

On a different note, plasma membrane-located CB_2 is internalized upon agonist stimulation and slowly recycled back to the cell surface via a Rab11-dependent pathway, while rapid recycling, via Rab4, does not occur.[40] Moreover, in the case of CB_2, not all receptors are recycled, and chronic agonist stimulation does not promote switching from recycling to degradative pathways, supporting the hypothesis of a putative

dx.doi.org/10.1021/bi500632a | Biochemistry 2014, 53, 4990−4999

role of sequestration of the CB_2 receptor to the cytoplasm following internalization.[40]

Our results, together with those of others,[12] add further complexity to the CB_2 receptor pharmacology and argue for careful consideration of receptor localization in the development of CB_2-based therapeutic agents. Moreover, because 2-AG is intracellularly produced "on demand",[41] its first target may be intracellularly located CB_2, which may be relevant both in physiological states and in pathologies with an increased level of production of endocannabinoids.

■ ASSOCIATED CONTENT

Supporting Information

Evidence of negligible effects of extracellular anandamide on CB_2-expressing U2OS cells or untransfected U2OS cells, insignificant responses produced by microinjected anandamide in untransfected U2OS cells is provided as supplemental data, and insignificant Ca^{2+} responses to extracellular or intracellular administration of WIN55,212-2 in untransfected U2OS cells. This material is available free of charge via the Internet at http://pubs.acs.org.

■ AUTHOR INFORMATION

Corresponding Authors

*Center for Substance Abuse Research, Temple University School of Medicine, 3500 N. Broad St., Room 848, Philadelphia, PA 19140. E-mail: ebrailou@temple.edu. Telephone: (215) 707-2791. Fax: (215) 707-9890.

*Center for Substance Abuse Research, Temple University School of Medicine, 3500 N. Broad St., Room 852, Philadelphia, PA 19140. E-mail: mabood@temple.edu. Telephone: (215) 707-2638. Fax: (215) 707-6661.

Author Contributions

G.C.B. and E.D. contributed equally to this work.

Funding

This work was supported by National Institutes of Health Grants HL090804 (to E.B.) and DA035926 and DA023204 (to M.E.A.).

Notes

The authors declare no competing financial interests.

■ ACKNOWLEDGMENTS

We thank Drs. Marc Caron and Lawrence S. Barak (Duke University) for providing the CB_2-U2OS cell line and the CB_2-GFP cDNA.

■ ABBREVIATIONS

2-AG, 2-arachidonoyl glycerol; $[Ca^{2+}]_i$, intracellular Ca^{2+} concentration; CB_2-U2OS, CB_2-β-arrestin 2-green fluorescent protein-U2OS; CTX, cholera toxin; DMEM, Dulbecco's modified Eagle's medium; D-SP, D-[Trp7,9,10]-substance P; EGTA, ethylene glycol tetraacetic acid; GFP, green fluorescent protein; GPCR, G protein-coupled receptor; HBSS, Hank's balanced salt solution; IP_3R, inositol 1,4,5-trisphosphate receptor; MAPK, mitogen-activated protein kinase; NAADP, nicotinic acid adenine dinucleotide phosphate; PTX, pertussis toxin; RFP, red fluorescent protein.

■ REFERENCES

(1) Pertwee, R. G., Howlett, A. C., Abood, M. E., Alexander, S. P., Di Marzo, V., Elphick, M. R., Greasley, P. J., Hansen, H. S., Kunos, G., Mackie, K., Mechoulam, R., and Ross, R. A. (2010) International Union of Basic and Clinical Pharmacology. LXXIX. Cannabinoid receptors and their ligands: Beyond CB_1 and CB_2. *Pharmacol. Rev. 62*, 588−5631.

(2) Anand, P., Whiteside, G., Fowler, C. J., and Hohmann, A. G. (2009) Targeting CB2 receptors and the endocannabinoid system for the treatment of pain. *Brain Res. Rev. 60*, 255−266.

(3) Cabral, G. A., and Griffin-Thomas, L. (2009) Emerging role of the cannabinoid receptor CB2 in immune regulation: Therapeutic prospects for neuroinflammation. *Expert Rev. Mol. Med. 11*, e3.

(4) Riether, D. (2012) Selective cannabinoid receptor 2 modulators: A patent review 2009−present. *Expert Opin. Ther. Pat. 22*, 495−510.

(5) Ruhl, T., Deuther-Conrad, W., Fischer, S., Gunther, R., Hennig, L., Krautscheid, H., and Brust, P. (2012) Cannabinoid receptor type 2 (CB2)-selective N-aryl-oxadiazolyl-propionamides: Synthesis, radiolabelling, molecular modelling and biological evaluation. *Org. Med. Chem. Lett. 2*, 32.

(6) Atwood, B. K., and Mackie, K. (2010) CB2: A cannabinoid receptor with an identity crisis. *Br. J. Pharmacol. 160*, 467−479.

(7) Atwood, B. K., Wager-Miller, J., Haskins, C., Straiker, A., and Mackie, K. (2012) Functional selectivity in CB_2 cannabinoid receptor signaling and regulation: Implications for the therapeutic potential of CB_2 ligands. *Mol. Pharmacol. 81*, 250−263.

(8) Onaivi, E. S., Ishiguro, H., Gu, S., and Liu, Q. R. (2012) CNS effects of CB2 cannabinoid receptors: Beyond neuro-immuno-cannabinoid activity. *J. Psychopharmacol. 26*, 92−103.

(9) Liu, Q. R., Pan, C. H., Hishimoto, A., Li, C. Y., Xi, Z. X., Llorente-Berzal, A., Viveros, M. P., Ishiguro, H., Arinami, T., Onaivi, E. S., and Uhl, G. R. (2009) Species differences in cannabinoid receptor 2 (CNR2 gene): Identification of novel human and rodent CB2 isoforms, differential tissue expression and regulation by cannabinoid receptor ligands. *Genes Brain Behav. 8*, 519−530.

(10) Bingham, B., Jones, P. G., Uveges, A. J., Kotnis, S., Lu, P., Smith, V. A., Sun, S. C., Resnick, L., Chlenov, M., He, Y., Strassle, B. W., Cummons, T. A., Piesla, M. J., Harrison, J. E., Whiteside, G. T., and Kennedy, J. D. (2007) Species-specific in vitro pharmacological effects of the cannabinoid receptor 2 (CB2) selective ligand AM1241 and its resolved enantiomers. *Br. J. Pharmacol. 151*, 1061−1070.

(11) Urban, J. D., Clarke, W. P., von Zastrow, M., Nichols, D. E., Kobilka, B., Weinstein, H., Javitch, J. A., Roth, B. L., Christopoulos, A., Sexton, P. M., Miller, K. J., Spedding, M., and Mailman, R. B. (2007) Functional selectivity and classical concepts of quantitative pharmacology. *J. Pharmacol. Exp. Ther. 320*, 1−13.

(12) den Boon, F. S., Chameau, P., Schaafsma-Zhao, Q., van Aken, W., Bari, M., Oddi, S., Kruse, C. G., Maccarrone, M., Wadman, W. J., and Werkman, T. R. (2012) Excitability of prefrontal cortical pyramidal neurons is modulated by activation of intracellular type-2 cannabinoid receptors. *Proc. Natl. Acad. Sci. U.S.A. 109*, 3534−3539.

(13) De Petrocellis, L., Marini, P., Matias, I., Moriello, A. S., Starowicz, K., Cristino, L., Nigam, S., and Di Marzo, V. (2007) Mechanisms for the coupling of cannabinoid receptors to intracellular calcium mobilization in rat insulinoma β-cells. *Exp. Cell Res. 313*, 2993−3004.

(14) Sugiura, T., Kondo, S., Kishimoto, S., Miyashita, T., Nakane, S., Kodaka, T., Suhara, Y., Takayama, H., and Waku, K. (2000) Evidence that 2-arachidonoylglycerol but not N-palmitoylethanolamine or anandamide is the physiological ligand for the cannabinoid CB2 receptor. Comparison of the agonistic activities of various cannabinoid receptor ligands in HL-60 cells. *J. Biol. Chem. 275*, 605−612.

(15) Zoratti, C., Kipmen-Korgun, D., Osibow, K., Malli, R., and Graier, W. F. (2003) Anandamide initiates Ca^{2+} signaling via CB2 receptor linked to phospholipase C in calf pulmonary endothelial cells. *Br. J. Pharmacol. 140*, 1351−1362.

(16) Yu, J., Deliu, E., Zhang, X. Q., Hoffman, N. E., Carter, R. L., Grisanti, L. A., Brailoiu, G. C., Madesh, M., Cheung, J. Y., Force, T., Abood, M. E., Koch, W. J., Tilley, D. G., and Brailoiu, E. (2013) Differential Activation of Cultured Neonatal Cardiomyocytes by Plasmalemmal Versus Intracellular G Protein-coupled Receptor 55. *J. Biol. Chem. 288*, 22481−22492.

(17) Brailoiu, G. C., Oprea, T. I., Zhao, P., Abood, M. E., and Brailoiu, E. (2011) Intracellular cannabinoid type 1 (CB1) receptors are activated by anandamide. *J. Biol. Chem. 286*, 29166−29174.
(18) Deliu, E., Brailoiu, G. C., Eguchi, S., Hoffman, N. E., Rabinowitz, J. E., Tilley, D. G., Madesh, M., Koch, W. J., and Brailoiu, E. (2014) Direct evidence of intracrine angiotensin II signaling in neurons. *Am. J. Physiol. 306*, C736−C744.
(19) Deliu, E., Brailoiu, G. C., Mallilankaraman, K., Wang, H., Madesh, M., Undieh, A. S., Koch, W. J., and Brailoiu, E. (2012) Intracellular endothelin type B receptor-driven Ca^{2+} signal elicits nitric oxide production in endothelial cells. *J. Biol. Chem. 287*, 41023−41031.
(20) Grynkiewicz, G., Poenie, M., and Tsien, R. Y. (1985) A new generation of Ca^{2+} indicators with greatly improved fluorescence properties. *J. Biol. Chem. 260*, 3440−3450.
(21) Bowman, E. J., Siebers, A., and Altendorf, K. (1988) Bafilomycins: A class of inhibitors of membrane ATPases from microorganisms, animal cells, and plant cells. *Proc. Natl. Acad. Sci. U.S.A. 85*, 7972−7976.
(22) Kunz, J. B., Schwarz, H., and Mayer, A. (2004) Determination of four sequential stages during microautophagy in vitro. *J. Biol. Chem. 279*, 9987−9996.
(23) Wang, T., Ming, Z., Xiaochun, W., and Hong, W. (2011) Rab7: Role of its protein interaction cascades in endo-lysosomal traffic. *Cell. Signalling 23*, 516−521.
(24) Mukai, H., Munekata, E., and Higashijima, T. (1992) G protein antagonists. A novel hydrophobic peptide competes with receptor for G protein binding. *J. Biol. Chem. 267*, 16237−16243.
(25) Naylor, E., Arredouani, A., Vasudevan, S. R., Lewis, A. M., Parkesh, R., Mizote, A., Rosen, D., Thomas, J. M., Izumi, M., Ganesan, A., Galione, A., and Churchill, G. C. (2009) Identification of a chemical probe for NAADP by virtual screening. *Nat. Chem. Biol. 5*, 220−226.
(26) Jalink, K., and Moolenaar, W. H. (2010) G protein-coupled receptors: The inside story. *BioEssays 32*, 13−16.
(27) Zhu, T., Gobeil, F., Vazquez-Tello, A., Leduc, M., Rihakova, L., Bossolasco, M., Bkaily, G., Peri, K., Varma, D. R., Orvoine, R., and Chemtob, S. (2006) Intracrine signaling through lipid mediators and their cognate nuclear G-protein-coupled receptors: A paradigm based on PGE2, PAF, and LPA1 receptors. *Can. J. Physiol. Pharmacol. 84*, 377−391.
(28) Benard, G., Massa, F., Puente, N., Lourenco, J., Bellocchio, L., Soria-Gomez, E., Matias, I., Delamarre, A., Metna-Laurent, M., Cannich, A., Hebert-Chatelain, E., Mulle, C., Ortega-Gutierrez, S., Martin-Fontecha, M., Klugmann, M., Guggenhuber, S., Lutz, B., Gertsch, J., Chaouloff, F., Lopez-Rodriguez, M. L., Grandes, P., Rossignol, R., and Marsicano, G. (2012) Mitochondrial CB_1 receptors regulate neuronal energy metabolism. *Nat. Neurosci. 15*, 558−564.
(29) Howlett, A. C., Barth, F., Bonner, T. I., Cabral, G., Casellas, P., Devane, W. A., Felder, C. C., Herkenham, M., Mackie, K., Martin, B. R., Mechoulam, R., and Pertwee, R. G. (2002) International Union of Pharmacology. XXVII. Classification of cannabinoid receptors. *Pharmacol. Rev. 54*, 161−202.
(30) Glass, M., and Felder, C. C. (1997) Concurrent stimulation of cannabinoid CB1 and dopamine D2 receptors augments cAMP accumulation in striatal neurons: Evidence for a Gs linkage to the CB1 receptor. *J. Neurosci. 17*, 5327−5333.
(31) Lauckner, J. E., Hille, B., and Mackie, K. (2005) The cannabinoid agonist WIN55,212-2 increases intracellular calcium via CB1 receptor coupling to Gq/11 G proteins. *Proc. Natl. Acad. Sci. U.S.A. 102*, 19144−19149.
(32) Sugiura, T., Kodaka, T., Kondo, S., Nakane, S., Kondo, H., Waku, K., Ishima, Y., Watanabe, K., and Yamamoto, I. (1997) Is the cannabinoid CB1 receptor a 2-arachidonoylglycerol receptor? Structural requirements for triggering a Ca^{2+} transient in NG108-15 cells. *J. Biochem. 122*, 890−895.
(33) Sugiura, T., Kodaka, T., Kondo, S., Tonegawa, T., Nakane, S., Kishimoto, S., Yamashita, A., and Waku, K. (1996) 2-Arachidonoylglycerol, a putative endogenous cannabinoid receptor ligand, induces rapid, transient elevation of intracellular free Ca^{2+} in neuroblastoma x glioma hybrid NG108-15 cells. *Biochem. Biophys. Res. Commun. 229*, 58−64.
(34) Shoemaker, J. L., Ruckle, M. B., Mayeux, P. R., and Prather, P. L. (2005) Agonist-directed trafficking of response by endocannabinoids acting at CB2 receptors. *J. Pharmacol. Exp. Ther. 315*, 828−838.
(35) Irannejad, R., Tomshine, J. C., Tomshine, J. R., Chevalier, M., Mahoney, J. P., Steyaert, J., Rasmussen, S. G., Sunahara, R. K., El-Samad, H., Huang, B., and von Zastrow, M. (2013) Conformational biosensors reveal GPCR signalling from endosomes. *Nature 495*, 534−538.
(36) Deliu, E., Tica, A. A., Motoc, D., Brailoiu, G. C., and Brailoiu, E. (2011) Intracellular angiotensin II activates rat myometrium. *Am. J. Physiol. 301*, C559−C565.
(37) Cosker, F., Cheviron, N., Yamasaki, M., Menteyne, A., Lund, F. E., Moutin, M. J., Galione, A., and Cancela, J. M. (2010) The ecto-enzyme CD38 is a nicotinic acid adenine dinucleotide phosphate (NAADP) synthase that couples receptor activation to Ca^{2+} mobilization from lysosomes in pancreatic acinar cells. *J. Biol. Chem. 285*, 38251−38259.
(38) Kim, S. Y., Cho, B. H., and Kim, U. H. (2010) CD38-mediated Ca^{2+} signaling contributes to angiotensin II-induced activation of hepatic stellate cells: Attenuation of hepatic fibrosis by CD38 ablation. *J. Biol. Chem. 285*, 576−582.
(39) Davis, L. C., Morgan, A. J., Ruas, M., Wong, J. L., Graeff, R. M., Poustka, A. J., Lee, H. C., Wessel, G. M., Parrington, J., and Galione, A. (2008) Ca^{2+} signaling occurs via second messenger release from intraorganelle synthesis sites. *Curr. Biol. 18*, 1612−1618.
(40) Grimsey, N. L., Goodfellow, C. E., Dragunow, M., and Glass, M. (2011) Cannabinoid receptor 2 undergoes Rab5-mediated internalization and recycles via a Rab11-dependent pathway. *Biochim. Biophys. Acta 1813*, 1554−1560.
(41) Hashimotodani, Y., Ohno-Shosaku, T., Tanimura, A., Kita, Y., Sano, Y., Shimizu, T., Di Marzo, V., and Kano, M. (2013) Acute inhibition of diacylglycerol lipase blocks endocannabinoid-mediated retrograde signalling: Evidence for on-demand biosynthesis of 2-arachidonoylglycerol. *J. Physiol. 591*, 4765−4776.